



Enhanced adsorption and recovery of Cu(II) and Fe(II) ions from wastewater using waste cellulose-loaded Mg(OH)₂ composite

M. Al-Mutair ^a, Md. Abu Taleb ^a, Mukarram Zubair ^b,
Rajeev Kumar ^a, and M.A. Barakat ^{a,c*}



CrossMark

^a Department of Environment, Faculty of Environmental Sciences,
King Abdulaziz University, Jeddah-21589, Saudi Arabia

^b Department of Environmental Engineering, Imam Abdulrahman Bin Faisal University, Saudi Arabia

Abstract

In this work, Mg(OH)₂ functionalized cellulose waste (CW@Mg(OH)₂) composite was prepared. The CW@Mg(OH)₂ composite was utilized for the adsorption of Cu(II) and Fe(II) ions from water and waste sludge streams. The characterization results indicated the successful formation of Mg(OH)₂ onto cellulose waste surface with high crystallinity and abundant surface functionalities (OH, C-O, and C-OH), which enhanced the removal % of heavy metals. At optimized adsorption conditions, the maximum monolayer adsorption capacity of CW@Mg(OH)₂ composite was 488 mg/g for Cu(II) and 510 mg/g Fe(II) at metal concentrations 400 mg/L with solution pH of ≥ 5.2 for both metal ions by 300 min. at 25 °C of system temperature. The experimental data was fitted to the recognized nonlinear isotherm and kinetic models. Energetically, the removal of Cu(II) and Fe(II) ions using CW@Mg(OH)₂ composite was impulsive and endothermic in nature. The adsorption mechanism of heavy metals onto CW@Mg(OH)₂ composite is mainly associated with surface adsorption, chemical, and hydrogen bonding due to surface functionalities as confirmed by FTIR. The CW@Mg(OH)₂ composite was investigated for the recovery of metal ions from microwave-digested sewage sludge and showed a removal % of (21 and 16 %) for iron and copper, respectively. The prepared CW@Mg(OH)₂ composite is cost-effective, stable, promising and effective for decontaminating heavy metals from wastewater.

Keywords: Wastewater, treatment, adsorption, recovery, Cu(II), Fe(II), CW@Mg(OH)₂.

1. Introduction

The rapid industrial advancement has led to increased wastewater discharge to environmental bodies. In this context, water pollution associated with the existence of hazardous metals such as copper, lead, iron, and arsenic poses a serious and devastating impact on the environment [1]. These heavy metals can enter waterways through different industrial activities such as mining, manufacturing, and agricultural runoff containing pesticides etc. [2]. Additionally, deteriorating lead pipes and corrosion of metal infrastructure can leach heavy metals into drinking water [3]. The excessive presence of heavy metals, including (Fe, Pb, and Cu) in drinking water subsequently causes severe human health issues, including damage to the human nervous system, learning disabilities, behavioural problems, vomiting, stomach cramps, etc. [4]. As per the World Health Organization (WHO) regulations, the allowable concentration of Fe, Cu, and Pb in water bodies should be 0.3, 2.0, and 0.01 mg/L, respectively [5]. Therefore, it is essential to effectively decontaminate and purify wastewater. Combating heavy metal contamination in water requires an appropriate treatment method. Numerous physical and chemical remediation techniques exist to remove heavy metal contamination, including adsorption, ion-exchange, membrane filtration, coagulation-flocculation, etc. [6][7]. These methods have some merits and demerits that limit their suitability for wastewater purification applications [8][9]. Among all studies methods, the adsorption is considered an easy and efficient technique to extract toxic metal ions from wastewater [10]. This is due to several factors, including high removal efficiency, low cost, easy operation, broad selectivity, and particularly in case of mixed contamination [11] [12]. However, the cost of the adsorbent material and low regeneration

*Corresponding author e-mail: mabarakat@gmail.com; (M.A. Barakat)

Received date 28 August 2024; revised date 16 October 2024; accepted date 25 October 2024

DOI: 10.21608/ejchem.2024.316094.10282

©2025 National Information and Documentation Center (NIDOC)

performance limit its potential for commercial applications [13]. Therefore, scientists are exerting efforts to design low-cost and sustainable adsorbents to effectively remove the heavy metals in wastewater.

During the past couple of decades, the utilization of low-cost adsorbent materials for water purification has received enormous interest [14]. Specifically, cellulose-based materials received significant attention due to their abundance, biodegradability, and less toxicity than other industrial wastes [15]. Cellulose is a low-cost adsorbent material, but its application is still limited due to its low affinity towards heavy metals and low regeneration performance. Therefore, the functionalization of cellulose-based materials may be expected to improve physicochemical characteristics and thus increase the adsorption capacity for heavy metals [16]. For example, office paper waste integrated with chitosan resulted in an aerogel exhibiting improved physical and chemical properties, including high mechanical stability and acid resistance, with a higher sorption capacity for Cu(II) of around 156.3 mg/g [17]. In another work, the waste newspaper was used as a low-cost matrix loaded with graphene oxide. The author reported promising removal of Pb²⁺, Ni²⁺, and Cd²⁺, with adsorption capacities of 75.41 mg/g, 29.04 mg/g, and 31.35 mg/g, respectively. In addition, the graphene oxide-loaded newspaper waste showed promising removal efficiency for lignin and COD in bleaching effluent indicating economical and promising material for enhanced adsorption of heavy metals [18]. Similarly, carboxymethylation of textile waste fabrics exhibited an excellent affinity for Cd(II) ions and showed up to 70% uptake of Cd(II) from water using a fixed bed column [19]. Previous studies revealed that the functionalization of adsorbent using magnesium is a promising approach [20]. This is associated with ease in synthesis and abundance of magnesium reserves in natural sources including salt lakes, seawater, etc [20]. The low cost, ease of availability, and non-toxicity of magnesium are promising materials to functionalize with low-cost adsorbent material, which resulted in green adsorbent material with a strong affinity towards heavy metals [21]. Wang et al., [22] coupled microcrystalline cellulose (MCC) and magnesium hydroxide (Mg(OH)₂) to produce a novel composite for enhanced adsorption of Co(II) ions from water. The author reported that MCC-MH removed 97.67% of Co at pH 6-8 with an adsorption capacity of 153.84 mg/g. The MCC-MH indicated promising Co(II) ions removal after five consecutive regenerative cycles [22]. Similarly, silica-decorated with MgO and NiO nanoparticles was used to remove Zn²⁺, Cu²⁺, and Cr³⁺ from wastewater. The author observed that the presence of MgO and NiO in the silica matrix significantly lowered the adsorption rate, and Cr³⁺ removal was achieved in 2 minutes. In contrast, Cu(II) and Zn(II) maximum adsorption was attained in 30 and 60 minutes, respectively [23].

In this study, the waste paper as the source of cellulose was collected from the waste box in the waste treatment industrial laboratory of the Department of Environment, King Abdulaziz University (KAU), Jeddah, Saudi Arabia, and modified with magnesium hydroxides using the coprecipitation method. The resultant composite is characterized by Fourier transform infrared spectroscopy (FTIR), X-ray diffraction (XRD), and scanning electron microscopy (SEM) to evaluate the chemical functionalities, crystallinity, and surface structure. The cellulose waste magnesium hydroxide composite (CW@Mg(OH)₂) was investigated for the adsorption of Fe(II) and Cu(II) ions from water and wastewater. The influence of influential adsorption parameters such as solution pH, contact time, initial heavy metal concentration, and temperature was investigated. Kinetic and isotherm modeling was performed to evaluate the sorption nature and mechanism of CW@Mg(OH)₂. The prepared adsorbent was evaluated at optimized adsorption conditions for the extraction of heavy metals from digested sewage sludge wastewater samples to assess the potential application of CW@Mg(OH)₂ as a sustainable, economical, and efficient adsorbent to remove and recover heavy metal ions from wastewater streams. The prepared CW@Mg(OH)₂ composite was cost-effective, stable, promising, and effective in decontaminating heavy metals from wastewater.

2. Material and Methods

2.1 Reagents

The pure analytical grade of chemicals/reagents was used directly in this study. The sodium hydroxide (NaOH) and magnesium chloride hexahydrate (MgCl₂·6H₂O) were obtained from the Tianli Chemical Reagent Manufacturing Co., Ltd. (Tianjin, China). The metal salts such as ferrous sulfate (FeSO₄·7H₂O) and copper sulfate (CuSO₄·5H₂O) were collected from BHD Chemical, Poole, England. DR/6000 UV-visible spectrophotometer was used to analyze both the Fe(II) and Cu(II) solutions using (cat. 1037690) and CuVer 1 copper reagent (cat 2105869), respectively.

2.2 Synthesis of adsorbents

2.2.1 Preparation of cellulose waste (CW)

The cellulose waste (CW) was modified from the source of waste tissue paper. The waste tissue paper was collected from different waste boxes around the Department of Environment, King Abdulaziz University (KAU), Jeddah, Saudi Arabia. The tissue paper was sterilized using UV light for 2 hours and washed with hot and cold water. Finally, the sterilized tissue papers

were kept in the oven for 24 hours to dry at 105 °C. After that, the dried cellulose waste was ground with a grinding machine (Rebun, model # RE-2-006, China) and stored for further composite synthesis steps.

2.2.2 Cellulose waste@magnesium hydroxide composite (CW@Mg(OH)₂)

To prepare the composite, nearly 3.0 g of magnesium chloride hexahydrate (MgCl₂·6H₂O) was weighed and mixed with 70 mL of distilled water. Further 1.0 g of sterilized tissue paper cellulose was added in the same solution and continuously stirred to obtain a homogenous solution. The hydroxide precipitate was formed by adjusting pH at around 11 using 0.1M NaOH. The solution was transferred to a hydrothermal reactor for 4 h at 150 °C. The reactor was removed and cooled down to 25 °C. The CW@Mg(OH)₂ composite was separated, washed, and dried at 80 °C. Finally, the modified adsorbent was then ready for adsorption application.

2.2.3 Characterization of modified adsorbents

The surface structure of CW@Mg(OH)₂ composite was scanned via SEM (JEOL, Tokyo, Japan). The crystal structures of the adsorbents were recorded by PAN analytical X'Pert PRO 3040/60 XRD machine from the Netherlands. Fourier transform infrared spectrophotometer (FT-IR, Berlin, Germany) analyzed the surface functionalities of the CW@Mg(OH)₂ composite.

2.2.4 Batch adsorption studies

In this work, the batch adsorption experiments were conducted by taking 200 mg of CW@Mg(OH)₂ composite plastic vials containing precisely 20 mL of Cu(II) and Fe(II) solutions at fixed concentrations in separate conical flasks. A solution of 0.1 M HCl and 0.1M NaOH was used to adjust the pH of the solution. The residual of metal ions was filtered using polyethersulfone (PES) 0.22 m microfilters. After the adsorption of Cu(II) and Fe(II) onto CW@Mg(OH)₂ composite, the HACH DR-6000 spectrophotometer was used for determining the residual concentrations of Cu(II) and Fe(II) solutions at λ_{max} 560 nm for Cu(II) and λ_{max} 562 nm for Fe(II), respectively. The following equations were applied for the determination of adsorption capacity onto CW@Mg(OH)₂ composite;

$$R\% = (C_0 - C_t) / C_0 * 100 \quad (1)$$

$$q_e(\text{mg/g}) = (C_0 - C_e) V / m \quad (2)$$

$$q_t(\text{mg/g}) = (C_0 - C_t) V / m \quad (3)$$

Where R is the removal of heavy metals in %, q_e is the adsorption capacity of used metal ions at equilibrium in mg/g, q_t is the adsorption capacity of used metal ions at time t in mg/g, C_t is the remaining concentration of metal ions at time t in mg/L, C_e is the remaining concentration of metal ions at equilibrium in mg/L, C₀ is the initial concentration (25 to 1000 mg/L) of Cu(II) and Fe(II) ions in mg/L, V is the volume of solution in liters and m is the dry weight of CW@Mg(OH)₂ composite.

3. Results and Discussion

3.1. Characterization of CW@Mg(OH)₂ bio-composite

3.1.1 FTIR analysis

Fig. 1a shows the change in the chemical structure of CW@Mg(OH)₂ before and after the adsorption of Cu(II) and Fe(II) ions. The FTIR spectra of pristine CW@Mg(OH)₂ indicate the formation of abundant surface functional groups, including OH, C-O, and C-O-H. The broad peak appeared at 3258 cm⁻¹ which is attributed to the hydroxyl (OH) stretching vibration from Mg(OH)₂ nanorods [26]. The strong and sharp peak at 1023 cm⁻¹ corresponds to the C-O groups of cellulose. In addition, the peaks observed at 1412 and 1591 cm⁻¹ were associated with bending vibrations of water molecules adsorbed onto the surface of CW@Mg(OH)₂ [27]. The FTIR spectra of CW@Mg(OH)₂ after Cu(II) and Fe(II) adsorption significantly changed, indicating the reduction in peak intensities and the appearance of new peaks. For instance, the hydroxyl group peak at 3258.7 cm⁻¹ decreased to low intensity and almost disappeared after Cu(II) and Fe(II) adsorption. This is attributed to the strong interaction of hydroxyl groups on CW@Mg(OH)₂ with heavy metals forming hydrogen bonds. Moreover, the sharp peak at 1023 cm⁻¹ represents C-O groups that showed a decrease in intensity after Fe(II) adsorption. Interestingly, a new peak was observed below 600 cm⁻¹ after Cu(II) adsorption. This corresponds to the metal oxide formation (Cu-O, O-Cu-O) [28] after adsorption. The FTIR results confirm that the surface functional groups onto CW@Mg(OH)₂ composite are dominant for enhanced uptake of Cu(II) and Fe(II) ions via chemical interactions.

3.1.2. XRD analysis

The crystalline structure CW@Mg(OH)₂ composite is analyzed by X-ray diffraction, and the results are depicted in Fig. 1b. As shown, the characteristics peaks at 2 theta 16.7° and 23.88° is attributed to the index plane of (110) and (200) of cellulose component, respectively [29]. The peaks at 35.1°, 38.76°, 51.64°, 59.1° and 63.06° of index plane of (100), (101), (102), (110)

and (111), respectively [30]. These are the crystalline peaks of $\text{Mg}(\text{OH})_2$, which confirm the homogeneous decoration of crystalline $\text{Mg}(\text{OH})_2$ particles onto the surface of cellulose. This demonstrated that the prepared composite is highly crystalline, which may have been expected to facilitate the uptake of $\text{Cu}(\text{II})$ and $\text{Fe}(\text{II})$ ions. Previous studies investigated modified $\text{Mg}(\text{OH})_2$ composites for the remediation of heavy metals contamination and demonstrated similar conclusions [24] [31].

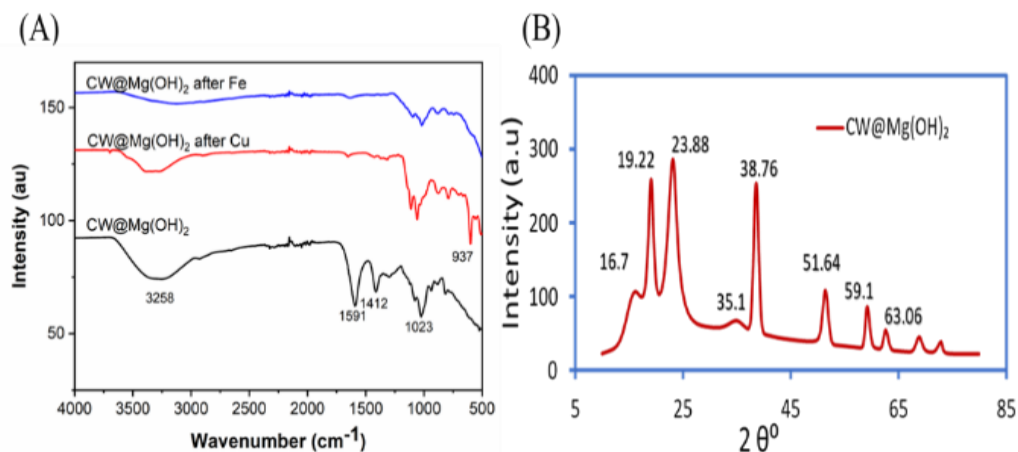


Fig. 1: (a) FTIR spectra of $\text{CW@Mg}(\text{OH})_2$ composite before and after adsorption (b) XRD of $\text{CW@Mg}(\text{OH})_2$ composite

3.1.3. SEM analysis

Fig. 2 and 3 show the changes in the surface structure of $\text{CW@Mg}(\text{OH})_2$ composite after adsorption of heavy metals. As seen in Fig. 2 (a-c), the microstructure of $\text{CW@Mg}(\text{OH})_2$ after $\text{Cu}(\text{II})$ adsorption at different magnifications (10, 50, and 100 μm) indicates the partial coverage of $\text{CW@Mg}(\text{OH})_2$ fibrous surface with $\text{Cu}(\text{II})$ particles. Li et al., [24] reported similar surface features after $\text{Cu}(\text{II})$ remediation using $\text{Fe}_3\text{O}_4@\text{Mg}(\text{OH})_2$ [24]. In contrast, the morphology of $\text{CW@Mg}(\text{OH})_2$ after $\text{Fe}(\text{II})$ adsorption, as displayed in Fig. 3 (a-c) at magnifications (50x-2500x) indicates a denser surface attributed to the complete coverage of $\text{CW@Mg}(\text{OH})_2$ composite surface with $\text{Fe}(\text{II})$ ions. This is a recognition of $\text{CW@Mg}(\text{OH})_2$ composite exhibited a strong affinity for $\text{Fe}(\text{II})$ ions compared to $\text{Cu}(\text{II})$ ions. This is mainly attributed to the existence of $\text{Mg}(\text{OH})_2$ on the $\text{CW@Mg}(\text{OH})_2$ surface, which chemically interacted with $\text{Fe}(\text{II})$ ions and then $\text{Cu}(\text{II})$. Shen et al. [25] reported high adsorption of $\text{Fe}(\text{II})$ compared to other heavy metals using $\text{Mg}(\text{OH})_2$ ultra-thin sheets within 6 min equilibrium time [25].

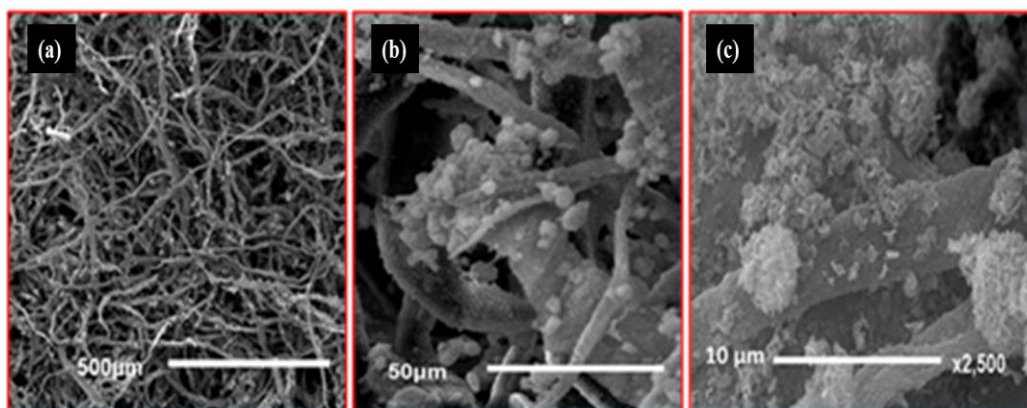


Fig. 2: SEM images of after $\text{Cu}(\text{II})$ adsorption-precipitation onto $\text{CW@Mg}(\text{OH})_2$ at (a) 50x, (b) 500x, (c) 2500x of magnification.

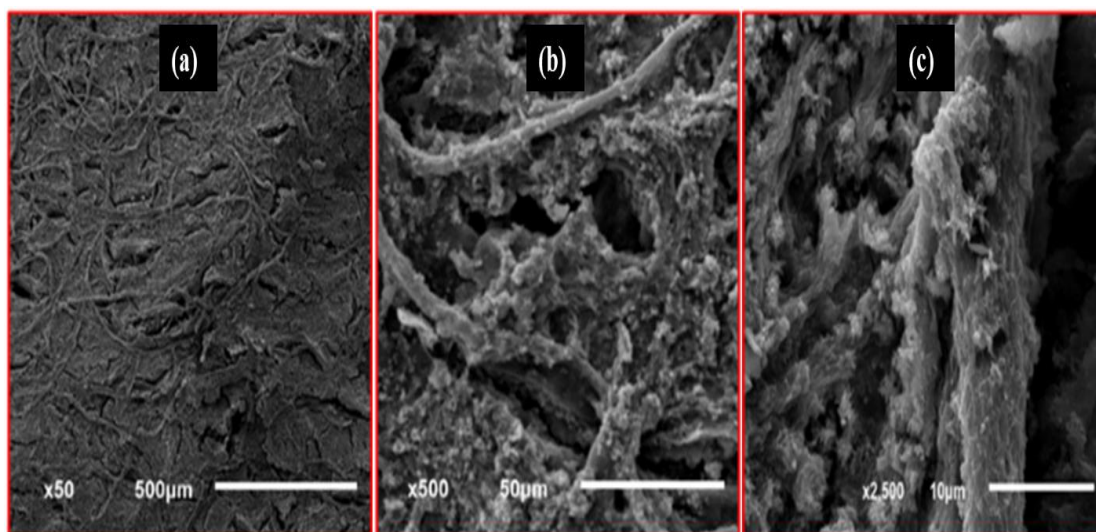


Fig. 3: SEM images of after Fe(II) adsorption-precipitation onto CW@Mg(OH)₂ at (a) 50x, (b) 500x, (c) 2500x of magnificant.

3.2. Adsorption performance of CW@Mg(OH)₂ bio-composite

3.2.1. pH Effect

The influence of initial pH on the sorption capacity of CW@Mg(OH)₂ for the removal of heavy metal ions was evaluated from a pH range of 2 to 5.3, and the results are displayed in Fig. 4. This demonstrated that for both heavy metals, the increase in pH from 2-5.3 linearly improved from 100 mg/g to approximately 250 mg/g. The maximum adsorption performance was achieved at pH >5, which is approximately 250 mg/g and 300 mg/g for Cu(II) and Fe(II), respectively. The low adsorption capacity of a composite at an acidic solution pH <5 is mainly associated with the formation of excess positively charged hydrogen ions onto the adsorbent surface, which act as competitive cations and reduce the sorption of Cu(II) and Fe(II). An increase in pH from 2-5 lowers the number of H⁺ ions, allows easy accessibility of heavy metals onto adsorbent surfaces and promotes interaction with surface functional groups via chemical and hydrogen bonding, as confirmed by FTIR analysis. Previous studies reported similar behaviour for the remediations of heavy metals using different adsorbents [32][33].

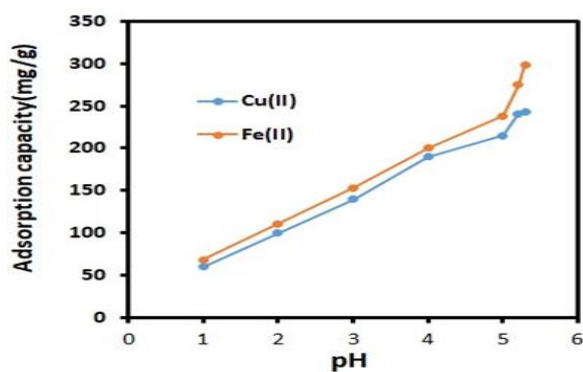


Fig.4: Effect of solution pH on adsorption-precipitation of Cu(II) and Fe(II) onto CW@Mg(OH)₂ composite (Conditions: concentration 400 mg/L, contact time 300 min., adsorbent mass 0.02 g).

3.2.2. Contact time effect and kinetic modelling

Fig. 5a displays the effect of the adsorption process time from 0 to 300 min for the remediation of heavy metals by CW@Mg(OH)₂ composite at an initial metal ion concentration of 400 mg/L and pH 5.2 for Cu(II), and 5.3 for Fe(II). As seen, the adsorption rate for both heavy metals was faster for the first 60 min, reaching a maximum sorption capacity of 100 mg/g for Cu(II) and Fe(II). Further, increasing the adsorption time to 150 min enhanced the sorption capacity to 200 mg/g. This is associated with the complete coverage of active sorption sites on the adsorbent surface, which strongly interact with heavy metals via physical and chemical interactions [34]. However, a negligible increase in adsorption capacity was observed after

300 min, indicating that within 300 min., equilibrium was achieved [35]. The maximum adsorption capacity of CW@Mg(OH)₂ composite for Cu(II) and Fe(II) was found to be 257 mg/g and 305 mg/g at 300 min. The high sorption capacity of composite for Fe(II) compared to Cu(II) is mainly associated with the formation of strong chemical interaction of composite surface functional groups with Fe(II) as confirmed by FTIR analysis after adsorption (Fig 1a). The rapid rate of adsorption of CW@Mg(OH)₂ composite followed by slow adsorption is mainly attributed to strong chemical interactions between heavy metals and active binding sorption sites of Mg(OH)₂ and oxygen functionalities [36], respectively.

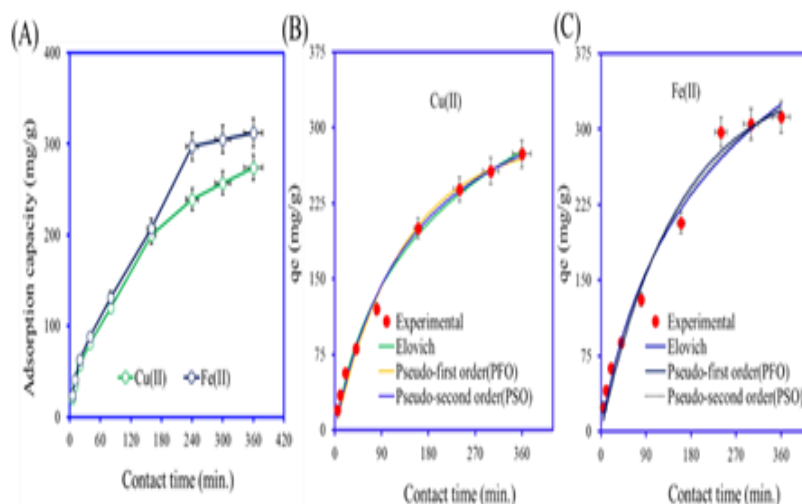


Fig. 5. (a) Effect of contact time of Cu(II) and Fe(II) of adsorption-precipitation onto CW@Mg(OH)₂ composite; (b c) kinetic plots of pseudo first order, second order and Elovich models (Conditions: concentration 400 mg/L, pH 5.2 for Cu(II), 5.3 for Fe(II); adsorbent mass 0.02 g).

To further evaluate the sorption behavior of Cu(II) and Fe(II) onto the surface of CW@Mg(OH)₂ composite, kinetic models such as Elovich, Pseudo-first order, and Pseudo-second order were fitted to the kinetic data. The R² and RMSE were among the criteria used to identify the best-fitted models. Fitting the models to the adsorption results in this study also took into account how closely the calculated and experimental results matched. The mathematical expression of RMSE and R² is as follows.

$$RMSE = \frac{1}{n-1} \sum_{i=1}^n (q_{exp} - q_{cal})^2 \quad (4)$$

$$R^2 = 1 - \frac{\sum (q_{exp} - q_{cal})^2}{\sum (q_{exp} - q_{cal})^2 + \sum (q_{exp} - q_{cal})^2} \quad (5)$$

Herein, Cu(II), and Fe(II) experimental and calculated adsorption capacities are denoted as q^{exp} and q^{cal} (mg/g). The number of data points is represented by n . The non-linear plots and estimated parameters of respective kinetic models are presented in Fig. 5(b c) and Table 1, respectively. As shown, for the adsorption of Cu(II), the correlation coefficients (R²) for all applied models is >0.99 indicating good fitting involving both physical and chemical interactions [37]. In addition, the root mean square deviation (RMSE) for the Elovich model (RMSE=6.59) is found lower than that for pseudo-first-order (RMSE=9.074) and pseudo-second-order (RMSE= 7.576). Based on RMSE results, the interaction Cu(II) ions with the CW@Mg(OH)₂ composite surface can be well described by the Elovich model [37]. This is associated with chemisorption processes such as chemical and hydrogen bonding, which significantly facilitates the uptake of Cu(II) ions on CW@Mg(OH)₂ composite [38]. Similarly, the value of R² is >0.98 for the fitted model on Fe(II) kinetic data. The values of RMSE are found in the range of PFO>PSO>Elovich, which suggests that the sorption of Fe(II) ions onto the CW@Mg(OH)₂ composite is mainly governed by chemical interactions. Interestingly, the adsorption rate as estimated using a pseudo-first-order model (Table 1) is slightly lower for Fe(II) ($k_1=0.006 \text{ min}^{-1}$) than Cu(II) ($k_1=0.007 \text{ min}^{-1}$), indicating fast and better affinity of composite for Fe(II) than Cu(II). This is mainly associated with stronger chemical interactions involved between surface functionalities (OH,C-O) of composite and Fe(II) ions.

Table 1. Kinetics parameters for the adsorption of Cu(II) and Fe(II) onto CW@Mg(OH)₂ composite

Kinetic model	Parameters	Cu(II)	Fe(II)
Pseudo-first order: $q_t = qe \left(1 - e^{(-k_1 t)} \right) \quad (6)$	q _e (mg/g) (exp.)	274.00	312.00
	q _i (mg/g) (cal.)	287.309	352.38
	k ₁ (min ⁻¹)	0.00762	0.00647
	R ²	0.990871	0.98281
	RMSE	9.074170	14.69
Pseudo-second order: $q_t = \frac{q_e^2 k_2 t}{k_2 (q_e) t + 1} \quad (7)$	q _e (mg/g) (cal.)	388.5610	491.57
	k ₂ (g/mg min ⁻¹)	1.68383	1.068
	R ²	0.993636	0.9839
	RMSE	7.576080	14.21
Elovich model: $q_t = \frac{1}{\beta} \ln(\alpha \beta t) \quad (8)$	a (mg/g min ⁻¹)	3.0874440	3.041
	β (mg/g)	0.0084718	0.0064
	R ²	0.9951756	0.9849
	RMSE	6.5967572	13.764

Table 2: Isotherm parameters for the Cu(II) and Fe(II) adsorption onto CW@Mg(OH)₂ composite

Isotherm model	Parameters	Cu(II)	Fe(II)
Langmuir $q_e = \frac{q_m k_L C_e}{1 + k_L C_e} \quad (9)$	q _m (mg/g)	488.00	510.00
	K _L (L/mg)	0.0044	0.0045
	R ²	0.9988	0.9990
	RMSE	5.8515	5.7641
Freundlich $q_e = k_F C_e^{\frac{1}{n}} \quad (10)$	N	10.403	11.504
	K _F (mg/g)	15.1345	2.3543
	R ²	0.9895	0.9963
	RMSE	9.219	11.208
Temkin $q_e = b_T * \ln(K_T * C_e) \quad (11)$	bt (J/mg)	20.35	21.3400
	K _T (L/mg)	0.160003	0.17000
	R ²	0.889724	0.89825
	RMSE	50.15803	59.1509
Redlich-Peterson $q_e = \frac{K_{RP} C_e}{1 + a_{RP} C_e^{n_{RP}}} \quad (12)$	K _{RP} (L/g)	3.9343	4.7284
	α _{RP} (L/mg)	0.00924	0.01224
	B	0.01015	0.84664
	R ²	0.9982	0.99915
	RMSE	4.4885	5.39855

3.2.3. Initial metal concentration effect and isotherm modeling

Fig. 6a shows the influence of change in initial metal (Cu and Fe) concentration (50-1000 mg/L) on the adsorption capacity of CW@Mg(OH)₂ composite at pH 5.2 for Cu(II), 5.3 for Fe(II), contact time 300 min, and temperature 30 °C. As seen, the rise in initial metal ions concentration resulted in linear enhancement in the adsorption capacity of the composite. For instance, the adsorption capacity of CW@Mg(OH)₂ composite for Cu(II) and Fe(II) significantly increased from 40-450 mg/g when the initial metal concentration rose from 25 to 1000 mg/L. The increase in sorption performance at elevated metal ions concentration is mainly associated with increased mass transfer phenomena due to the presence of abundant metal ions in solution [39]. This resulted in complete coverage of the active sorption sites in the composite surface. The results are consistent with previous studies that investigated the adsorption performance of metal ions using different adsorbents [10][40].

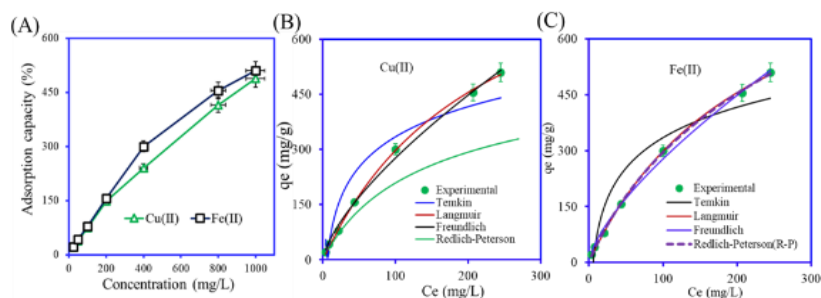


Fig. 6. (a) Effect of initial concentration of Cu(II) and Fe(II) of adsorption-precipitation onto CW@Mg(OH)₂ composite (b c) nonlinear isotherms plots for the adsorption of Cu(II) and Fe(II) onto CW@Mg(OH)₂ composite (Conditions: concentration 400 mg/L, pH 5.2 for Cu(II), 5.3 for Fe(II); contact time 5 hrs, adsorbent mass 0.02 g).

The adsorption mechanism of heavy metals onto CW@Mg(OH)₂ composite was further determined using isotherm models. In this work, three widely used models, Langmuir, Freundlich, and Redlich Peterson, were fitted to equilibrium data, and their non-linear plots are depicted in Fig. 6(b c). The isotherm parameters are estimated using non-linear equations, and the results are listed in Table 2. It is observed that for the adsorption of Cu(II), the Langmuir and Redlich Peterson dominantly provide better fitting than Freundlich and Tempkin, with the highest R^2 values (0.998 for Cu(II)). Whereas for Fe(II), Langmuir, Freundlich and Redlich Peterson showed high R^2 value of 0.999. In addition, for both metal ions, the estimated RMSE for Redlich Peterson is found to be the lowest compared to Langmuir and Freundlich models. This indicated that the adsorption of both metal ions (Cu and Fe) can be well described by the Redlich-Peterson model. Interestingly, the value of β from the Redlich-Peterson model approached zero and unity for C(II) and Fe(II), respectively.

This implies that Cu(II) adsorption is mainly governed and dominated by monolayer adsorption. Similar behaviour was reported by Liu et al., [41] for the adsorption of Cu(II) using sodium alginate/carboxymethylcellulose/magnesium hydroxide hydrogels [41]. Meanwhile, for Fe(II), the adsorption mechanism predominantly involves multi-layers on the composite surface associated with chemical and physical interactions [42][43]. The maximum monolayer Cu(II) and Fe(II) adsorption capacities of 488 mg/g and 510 mg/g, respectively, for the CW@Mg(OH)₂ composite, were estimated at the initial metal concentration (400 mg/l), pH (5.2), contact time (300 min) and temperature (30 °C). The sorption capacity of CW@Mg(OH)₂ composite for Fe(II) was relatively greater than Cu(II) (Table 2). This further strengthens affinity of CW@Mg(OH)₂ composite surface functionalities with Fe(II) ions via chemical and physical interactions [44][45].

3.2.4. Temperature effect

The influence of adsorption temperature on the adsorption capacity of CW@Mg(OH)₂ composite for heavy metals was evaluated at temperatures ranging from 30 to 50 °C. The results are depicted in Fig. 7. It was shown that for both Cu(II) and Fe(II), the adsorption capacity of CW@Mg(OH)₂ composite improved with increasing process temperature. For example, for Cu(II) ions, the adsorption capacity of CW@Mg(OH)₂ composite was found to be 240 mg/g at 30 °C, which was increased to 275 mg/g when temperature increased to 50 °C. Similarly, in case of Fe(II), the adsorption capacity of the composite increased 300 mg/g to 351 mg/g when the temperature increased from 30 to 50 °C. The results confirmed that the adsorption process is endothermic and relatively favorable at higher temperatures.

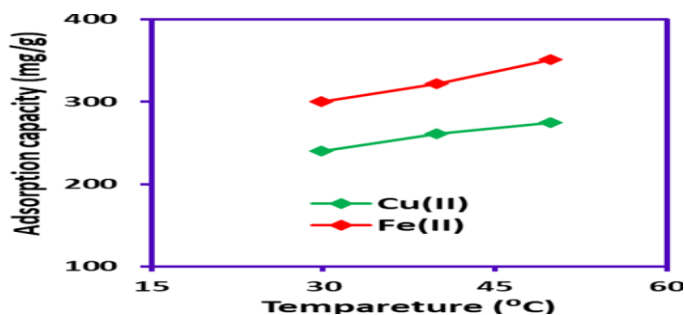


Fig.7: Effect of temperature of Cu(II) and Fe(II) adsorption-precipitation onto CW@Mg(OH)₂ composite (Conditions: concentration 400 mg/L, pH 5.2 for Cu(II), 5.3 for Fe(II); contact time 5 hrs; adsorbent mass 0.02 g).

3.2.5. Comparison with other adsorbents

The adsorption performance of CW@Mg(OH)₂ composite for the removal of Cu(II) and Fe(II) was compared with previously studied Mg(OH)₂ based composites and other low-cost sorbents, and the results are listed in Table 3. The results indicated that the composite fabricated in this work showed a comparatively higher adsorption performance of both metal ions (Cu and Fe) compared to various studies of Mg(OH)₂ based composites and other adsorbents. For instance, a composite of Sodium alginate decorated with carboxymethyl cellulose and magnesium hydroxide and magnesium hydroxide-supported activated carbon showed an adsorption capacity of 215.68 mg/g and 58.88 mg/g for Cu(II) which is almost 50-80% lower than CW@Mg(OH)₂ composite (488 mg/g). Moreover, the adsorption capacity of CW@Mg(OH)₂ composite for Fe(II) is almost 5-20 times higher than that of previously reported adsorbents (Table 3). The results clearly confirm that prepared CW@Mg(OH)₂ composite is an eco-friendly and promising material exhibiting superior affinity and high adsorption performance for heavy metals from wastewater.

Table 3: Comparison of adsorption capacity and parameters of Cu(II) and Fe(II) onto other adsorbent

Adsorbent	pH	Temperature (°C)	q _m (mg/g)		Ref
			Cu(II)	Fe(II)	
Sodium alginate/carboxymethylcellulose/magnesium hydroxide	5	25	215.68	-	[41]
Al-Alg/GO/AIOOH	5.5	30	83.0		[46]
Magnesium hydroxide-modified activated carbon	7	25	58.88	-	[47]
CMC/GO/PANI	5.3	30	247.69		[48]
Mg(OH) ₂ @GO-coated activated carbon fiber cloth	5	25	439.5	-	[36]
SiO ₂ /CuFe ₂ O ₄ /polyaniline	5.5	30	285.71	416.67	[49]
Activated clinoptilolite	3	-	-	104.0	[50]
Bentonite	-	-	-	16.65	[51]
E. coli biofilm supported on kaolin	3	-	-	16.5	[52]
Pretreated orange peel				18.19	[53]
Cellulose waste-Mg(OH) ₂ composite	5-5.3	30	488	510	This study

3.3. Microwave acid extraction of Cu(II) and Fe(II)

The extraction of Cu(II) and Fe(II) from sewage sludge was performed at different microwave temperatures (80-160 °C) and nitric acid ratio (5-20), and the results are displayed in Fig. 8(a b). As seen, at temperature 80 °C, a higher % extraction of Cu(II) of 23% was observed at 15:1 (HNO₃:HCl). As the microwave extraction temperature increased to 120 °C, the highest Cu(II) was found at 10:1 (HNO₃:HCl). In contrast, a further increase in microwave extraction temperature to 160 °C demonstrated a reduction in Cu(II) extraction to 21% at 20:1 (HNO₃:HCl). In the case of microwave extraction for Fe(II), the results as depicted in Figure 8b demonstrated that the % extraction of Fe(II) improved with increasing microwave temperature and decreasing HNO₃:HCl ratio. For instance, at 5:1 (HNO₃:HCl), the % extraction of Fe(II) was 21% at a microwave temperature of 80 °C, which was increased to 24% when the temperature enhanced to 160 °C at the same HNO₃:HCl ratio. The results confirmed that microwave temperature and HNO₃:HCl ratio significantly influence % extraction of Cu(II) and Fe(II) and appropriate conditions should be selected for high extraction of metal ions.

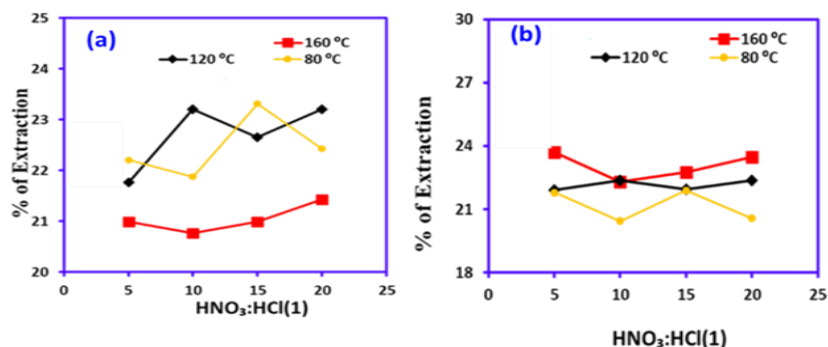


Fig. 8: Microwave extraction of (a) Cu(II) and (b) Fe(II) at varied temperatures and acid ratios.

3.4. Heavy metals removal from industrial sludge

The CW@Mg(OH)₂ composite was utilized for the remediation of heavy metals (Fe and Cu) in real digested sludge sample, and the results are shown in Fig. 9. The % composition of heavy metals in the digested sludge sample is shown in Table S1. The adsorption experiment was conducted at varied pH (5, 7, and 12) and fixed contact time (360 minutes), composite dosage (0.1 g), and temperature (30 °C). The adsorption results are shown in Fig. 9. As expected, the % removal of Fe and Cu ions increased with an increase in solution pH 5-12, associated with the precipitation of metal ions above pH>5. At all pH values, the uptake of heavy metals using CW@Mg(OH)₂ composite was found as Fe>Cu. At a pH value of 5, the % removal of Fe and Cu, was 24.5 and 16, which increased to 29 and 28 % when pH increased to 7. The results demonstrated that the prepared CW@Mg(OH)₂ composite exhibits great potential to effectively recover precious heavy metals from real wastewater streams.

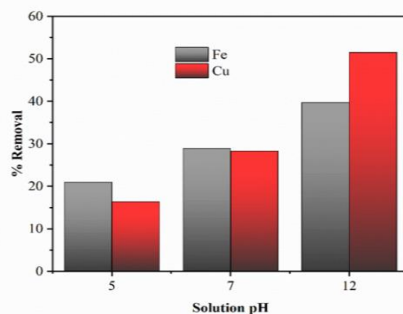


Fig. 9: Recovery of heavy metals from digested sewage sludge using CW@(MgOH)₂

4. Conclusions

Mg(OH)₂-nanorods decorated cellulose waste (CW@Mg(OH)₂) composite was synthesized using the co-precipitation method. The CW@Mg(OH)₂ composite was used for the remediation of Cu(II) and Fe(II) ions from water and waste sludge streams. The characterization results indicated the successful formation of Mg(OH)₂-nanorods onto cellulose waste surfaces with high crystallinity and abundant surface functionalities (OH, C-O, and C-OH), which may have been expected to enhance the uptake of heavy metals from water. The adsorption of heavy metals using CW@Mg(OH)₂ composite was influenced by initial solution pH, initial metal concentration, contact time, and temperature. The kinetic results were better demonstrated by the Elovich model, which indicates that chemisorption is the dominant mechanism. The Langmuir and Redlich-Peterson model showed higher fitting to equilibrium data for the adsorption of Cu(II) and Fe(II), which showed monolayer and multilayer adsorption. The maximum monolayer adsorption capacity for Cu(II) and Fe(II) was 488 mg/g and 510 mg/g, respectively. The adsorption of Cu(II) and Fe(II) was favorable at elevated temperatures and endothermic in nature. The adsorption mechanism of heavy metals onto CW@Mg(OH)₂ composite is mainly associated with surface adsorption and chemical and hydrogen bonding with surface functionalities as confirmed by FTIR and SEM analysis after adsorption. The composite showed % removal of (24.5 and 16) for Fe and Cu from real microwave-digested sewage sludge. The composite exhibited promising characteristics for heavy metals removal and can be utilized as a low-cost and sustainable material for the remediation of heavy metals contaminated water.

5. Conflicts of interest

There are no conflicts to declare.

6. Acknowledgments

This project was funded by the Deanship of Scientific Research (DSR) at King Abdulaziz University, Jeddah, under grant no. (GPIP:353-155-2024). The authors, therefore, acknowledge with thanks DSR for technical and financial support.

7. References

- [1] S. Mitra, A.J. Chakraborty, A.M. Tareq, T. Bin Emran, F. Nainu, A. Khusro, A.M. Idris, M.U. Khandaker, H. Osman, F.A. Alhumaydhi, J. Simal-Gandara, Impact of heavy metals on the environment and human health: Novel therapeutic insights to counter the toxicity, *J. King Saud Univ. - Sci.* 34 (2022) 101865. <https://doi.org/https://doi.org/10.1016/j.jksus.2022.101865>.
- [2] A. Alengebawy, S.T. Abdelkhalek, S.R. Qureshi, M.-Q. Wang, Heavy Metals and Pesticides Toxicity in Agricultural Soil and Plants: Ecological Risks and Human Health Implications., *Toxics* 9 (2021). <https://doi.org/10.3390/toxics9030042>.
- [3] D.-Q. Ng, J.-K. Lin, Y.-P. Lin, Lead release in drinking water resulting from galvanic corrosion in three-metal systems consisting of lead, copper and stainless steel, *J. Hazard. Mater.* 398 (2020) 122936. <https://doi.org/https://doi.org/10.1016/j.jhazmat.2020.122936>.
- [4] M. Jaishankar, T. Tseten, N. Anbalagan, B.B. Mathew, K.N. Beeregowda, Toxicity, mechanism and health effects of some heavy metals., *Interdiscip. Toxicol.* 7 (2014) 60–72. <https://doi.org/10.2478/intox-2014-0009>.
- [5] H.N. Muhammad Ekramul Mahmud, A.K.O. Huq, R. binti Yahya, The removal of heavy metal ions from wastewater/aqueous solution using polypyrrole-based adsorbents: a review, *RSC Adv.* 6 (2016) 14778–14791. <https://doi.org/10.1039/C5RA24358K>.
- [6] M.A. Hashim, S. Mukhopadhyay, J.N. Sahu, B. Sengupta, Remediation technologies for heavy metal contaminated groundwater, *J. Environ. Manage.* 92 (2011) 2355–2388. <https://doi.org/https://doi.org/10.1016/j.jenvman.2011.06.009>.
- [7] A. Selvi, A. Rajasekar, J. Theerthagiri, A. Ananthaselvam, K. Sathishkumar, J. Madhavan, P.K.S.M. Rahman, Integrated Remediation Processes Toward Heavy Metal Removal/Recovery From Various Environments-A Review , *Front. Environ. Sci.* 7 (2019). <https://www.frontiersin.org/articles/10.3389/fenvs.2019.00066>.
- [8] C. Zamora-Ledezma, D. Negrete-Bolagay, F. Figueroa, E. Zamora-Ledezma, M. Ni, F. Alexis, V.H. Guerrero, Heavy metal water pollution: A fresh look about hazards, novel and conventional remediation methods, *Environ. Technol. Innov.* 22 (2021) 101504. <https://doi.org/https://doi.org/10.1016/j.eti.2021.101504>.
- [9] R. Vidu, E. Matei, A.M. Predescu, B. Alhalaili, C. Pantilimon, C. Tarcea, C. Predescu, Removal of Heavy Metals from Wastewaters: A Challenge from Current Treatment Methods to Nanotechnology Applications, *Toxics* 8 (2020). <https://doi.org/10.3390/toxics8040101>.
- [10] N.A.A. Qasem, R.H. Mohammed, D.U. Lawal, Removal of heavy metal ions from wastewater: a comprehensive and critical review, *Npj Clean Water.* 4 (2021) 36. <https://doi.org/10.1038/s41545-021-00127-0>.
- [11] A. Hussain, S. Madan, R. Madan, Removal of Heavy Metals from Wastewater by Adsorption, in: M.K. Nazal, H. Zhao (Eds.), *IntechOpen, Rijeka*, 2021: p. Ch. 10. <https://doi.org/10.5772/intechopen.95841>.
- [12] S. Jadoun, J.P. Fuentes, B.F. Urbano, J. Yáñez, A review on adsorption of heavy metals from wastewater using conducting polymer-based materials, *J. Environ. Chem. Eng.* 11 (2023) 109226. <https://doi.org/https://doi.org/10.1016/j.jece.2022.109226>.
- [13] S. De Gisi, G. Lofrano, M. Grassi, M. Notarnicola, Characteristics and adsorption capacities of low-cost sorbents for wastewater treatment: A review, *Sustain. Mater. Technol.* 9 (2016) 10–40. <https://doi.org/https://doi.org/10.1016/j.susmat.2016.06.002>.
- [14] M. Bilal, I. Ihsanullah, M. Younas, M. Ul Hassan Shah, Recent advances in applications of low-cost adsorbents for the removal of heavy metals from water: A critical review, *Sep. Purif. Technol.* 278 (2021) 119510. <https://doi.org/https://doi.org/10.1016/j.seppur.2021.119510>.
- [15] M.N. Faiz Norraahim, N.A. Mohd Kasim, V.F. Knight, M.S. Mohamad Misenan, N. Janudin, N.A. Ahmad Shah, N. Kasim, W.Y. Wan Yusoff, S.A. Mohd Noor, S.H. Jamal, K.K. Ong, W.M. Zin Wan Yunus, Nanocellulose: a bioadsorbent for chemical contaminant remediation., *RSC Adv.* 11 (2021) 7347–7368. <https://doi.org/10.1039/d0ra08005e>.
- [16] B. Peng, Z. Yao, X. Wang, M. Crombeen, D.G. Sweeney, K.C. Tam, Cellulose-based materials in wastewater treatment of petroleum industry, *Green Energy Environ.* 5 (2020) 37–49. <https://doi.org/https://doi.org/10.1016/j.gee.2019.09.003>.
- [17] Z. Li, L. Shao, Z. Ruan, W. Hu, L. Lu, Y. Chen, Converting untreated waste office paper and chitosan into aerogel adsorbent for the removal of heavy metal ions, *Carbohydr. Polym.* 193 (2018) 221–227. <https://doi.org/https://doi.org/10.1016/j.carbpol.2018.04.003>.

- [18] H. Chen, Y. Meng, S. Jia, W. Hua, Y. Cheng, J. Lu, H. Wang, Graphene oxide modified waste newspaper for removal of heavy metal ions and its application in industrial wastewater, *Mater. Chem. Phys.* 244 (2020) 122692. <https://doi.org/https://doi.org/10.1016/j.matchemphys.2020.122692>.
- [19] J.K. Bediako, W. Wei, Y.-S. Yun, Conversion of waste textile cellulose fibers into heavy metal adsorbents, *J. Ind. Eng. Chem.* 43 (2016) 61–68. <https://doi.org/https://doi.org/10.1016/j.jiec.2016.07.048>.
- [20] A.M. Alkadhém, M.A.A. Elgzoly, S.A. Onaizi, Novel Amine-Functionalized Magnesium Oxide Adsorbents for CO₂ Capture at Ambient Conditions, *J. Environ. Chem. Eng.* 8 (2020) 103968. <https://doi.org/https://doi.org/10.1016/j.jece.2020.103968>.
- [21] H. Sugita, T. Oguma, J. Hara, M. Zhang, Y. Kawabe, Removal of Arsenate from Contaminated Water via Combined Addition of Magnesium-Based and Calcium-Based Adsorbents, *Sustainability*. 15 (2023). <https://doi.org/10.3390/su15054689>.
- [22] R. Wang, L. Deng, X. Fan, K. Li, H. Lu, W. Li, Removal of heavy metal ion cobalt (II) from wastewater via adsorption method using microcrystalline cellulose–magnesium hydroxide, *Int. J. Biol. Macromol.* 189 (2021) 607–617. <https://doi.org/https://doi.org/10.1016/j.ijbiomac.2021.08.156>.
- [23] S. Abuhatab, A. El-Qanni, H. Al-Qalaq, M. Hmoudah, W. Al-Zerei, Effective adsorptive removal of Zn²⁺, Cu²⁺, and Cr³⁺ heavy metals from aqueous solutions using silica-based embedded with NiO and MgO nanoparticles, *J. Environ. Manage.* 268 (2020) 110713. <https://doi.org/https://doi.org/10.1016/j.jenvman.2020.110713>.
- [24] J. Zhu, P. Li, B. Yang, S. Lan, W. Chen, D. Zhu, Facile fabrication of Fe₃O₄@Mg(OH)₂ magnetic composites and their application in Cu(II) ion removal, *RSC Adv.* 13 (2023) 33403–33412. <https://doi.org/10.1039/D3RA05961H>.
- [25] X. SHEN, Y. HUANG, H. SHAO, Y. WANG, Q. HAN, J. CHEN, B. LI, Y. ZHAI, Facile fabrication of spherical flower-like Mg(OH)₂ and its fast and efficient removal for heavy metal ions, *Trans. Nonferrous Met. Soc. China.* 32 (2022) 3149–3162. [https://doi.org/https://doi.org/10.1016/S1003-6326\(22\)66010-2](https://doi.org/https://doi.org/10.1016/S1003-6326(22)66010-2).
- [26] M. Zubair, M.S. Manzar, A. El-Qanni, H. Haroon, H.A. Alqahtani, M. Al-Ejji, N.D. Mu'azu, J.M. AlGhamdi, S.A. Haladu, D. Al-Hashim, S.Z. Ahmed, Biochar-layered double hydroxide composites for the adsorption of tetracycline from water: synthesis, process modeling, and mechanism, *Environ. Sci. Pollut. Res.* 30 (2023) 109162–109180. <https://doi.org/10.1007/s11356-023-29954-z>.
- [27] W. Wu, F. Zhang, Y. Li, L. Song, D. Jiang, R.-C. Zeng, S.C. Tjong, D.-C. Chen, Corrosion resistance of dodecanethiol-modified magnesium hydroxide coating on AZ31 magnesium alloy, *Appl. Phys. A.* 126 (2019) 8. <https://doi.org/10.1007/s00339-019-3150-3>.
- [28] M. Zubair, H.A. Aziz, I. Ihsanullah, M.A. Ahmad, M.A. Al-Harhi, Biochar supported CuFe layered double hydroxide composite as a sustainable adsorbent for efficient removal of anionic azo dye from water, *Environ. Technol. Innov.* 23 (2021) 101614. <https://doi.org/10.1016/j.eti.2021.101614>.
- [29] M. Nasir, M.A. Aziz, M. Zubair, N. Ashraf, T.N. Hussein, M.K. Allubli, M.S. Manzar, W. Al-Kutti, M. A. Al-Harhi, Engineered cellulose nanocrystals-based cement mortar from office paper waste: Flow, strength, microstructure, and thermal properties, *J. Build. Eng.* 51 (2022) 104345. <https://doi.org/https://doi.org/10.1016/j.jobte.2022.104345>.
- [30] G.W. Beall, E.-S.M. Duraia, F. El-Tantawy, F. Al-Hazmi, A.A. Al-Ghamdi, Rapid fabrication of nanostructured magnesium hydroxide and hydromagnesite via microwave-assisted technique, *Powder Technol.* 234 (2013) 26–31. <https://doi.org/https://doi.org/10.1016/j.powtec.2012.09.029>.
- [31] M. El Bouraie, A.A. Masoud, Adsorption of phosphate ions from aqueous solution by modified bentonite with magnesium hydroxide Mg(OH)₂, *Appl. Clay Sci.* 140 (2017) 157–164. <https://doi.org/https://doi.org/10.1016/j.clay.2017.01.021>.
- [32] Kumar R., Barakat, M.A., Taleb M.A. and Seliem M.K., 2020. A recyclable multifunctional graphene oxide/SiO₂@polyaniline microspheres composite for Cu(II) and Cr(VI) decontamination from wastewater. *J Clean Prod.* 268, 122290.
- [33] R.S. Brishti, R. Kundu, M.A. Habib, M.H. Ara, Adsorption of iron(III) from aqueous solution onto activated carbon of a natural source: Bombax ceiba fruit shell, *Results Chem.* 5 (2023) 100727. <https://doi.org/https://doi.org/10.1016/j.rechem.2022.100727>.
- [34] S.A. Abd El Aal, A.M. Abdelhady, N.A. Mansour, N.M. Hassan, F. Elbaz, E.K. Elmaghraby, Physical and chemical characteristics of hematite nanoparticles prepared using microwave-assisted synthesis and its application as adsorbent for Cu, Ni, Co, Cd and Pb from aqueous solution, *Mater. Chem. Phys.* 235 (2019) 121771. <https://doi.org/https://doi.org/10.1016/j.matchemphys.2019.121771>.
- [35] N. Hossain, S. Nizamuddin, K. Shah, Thermal-chemical modified rice husk-based porous adsorbents for Cu (II), Pb (II), Zn (II), Mn (II) and Fe (III) adsorption, *J. Water Process Eng.* 46 (2022) 102620. <https://doi.org/https://doi.org/10.1016/j.jwpe.2022.102620>.

- [36] X. Wang, J. Li, Q. Guo, M. Xu, X. Zhang, T. Li, Cation- π interaction in Mg(OH)₂@GO-coated activated carbon fiber cloth for rapid removal and recovery of divalent metal cations by flow-through adsorption, *Resour. Conserv. Recycl.* 188 (2023) 106648. <https://doi.org/https://doi.org/10.1016/j.resconrec.2022.106648>.
- [37] C. Zhao, C. Wang, Z. Wang, B. Wang, G. Yao, Y. Qiu, R. Yang, Study of the removal of Pb(II) and Ni(II) from aqueous solution by new nano-Mg(OH)₂/fly ash adsorbent materials, *New J. Chem.* 47 (2023) 10952–10966. <https://doi.org/10.1039/D3NJ01565C>.
- [38] L. Gong, Z. Yao, C. Zhu, X. Lian, B. He, L. Qu, W. Xiong, B. Yu, Synthesis of porous Mg(OH)₂ nanowires for phosphate removal from water, *Colloids Surfaces A Physicochem. Eng. Asp.* 676 (2023) 132137. <https://doi.org/https://doi.org/10.1016/j.colsurfa.2023.132137>.
- [39] A.A. khedr, M.E. Fawzy, H.M. Ahmed, S.O. Alshammari, M.A. El-Khateeb, Treatment of heavy metal ions from simulated water using adsorption process via modified iron magnetic nanocomposite, *Desalin. Water Treat.* 317 (2024) 100071. <https://doi.org/https://doi.org/10.1016/j.dwt.2024.100071>.
- [40] J. Li, X. Dong, X. Liu, X. Xu, W. Duan, J. Park, L. Gao, Y. Lu, Comparative Study on the Adsorption Characteristics of Heavy Metal Ions by Activated Carbon and Selected Natural Adsorbents, *Sustainability.* 14 (2022). <https://doi.org/10.3390/su142315579>.
- [41] Z. Liu, J. Zhao, A. Wang, H. Yuan, Y. Chi, Adsorption behavior and mechanism of Cu(II) by sodium alginate/carboxymethylcellulose/magnesium hydroxide (SC-MH) hydrogel, *Int. J. Biol. Macromol.* (2024) 134046. <https://doi.org/https://doi.org/10.1016/j.ijbiomac.2024.134046>.
- [42] J. Di, Z. Ruan, S. Zhang, Y. Dong, S. Fu, H. Li, G. Jiang, Adsorption behaviors and mechanisms of Cu(2+), Zn(2+) and Pb(2+) by magnetically modified lignite., *Sci. Rep.* 12 (2022) 1394. <https://doi.org/10.1038/s41598-022-05453-y>.
- [43] Z. Raji, A. Karim, A. Karam, S. Khalloufi, Adsorption of Heavy Metals: Mechanisms, Kinetics, and Applications of Various Adsorbents in Wastewater Remediation—A Review, *Waste.* 1 (2023) 775–805. <https://doi.org/10.3390/waste1030046>.
- [44] E. Kumar, A. Bhatnagar, W. Hogland, M. Marques, M. Sillanpää, Interaction of inorganic anions with iron-mineral adsorbents in aqueous media — A review, *Adv. Colloid Interface Sci.* 203 (2014) 11–21. <https://doi.org/https://doi.org/10.1016/j.cis.2013.10.026>.
- [45] P. Maneechakr, S. Karnjanakom, Adsorption behaviour of Fe(II) and Cr(VI) on activated carbon: Surface chemistry, isotherm, kinetic and thermodynamic studies, *J. Chem. Thermodyn.* 106 (2017) 104–112. <https://doi.org/https://doi.org/10.1016/j.jct.2016.11.021>.
- [46] Taleb M.A., Kumar R. and Barakat M.A., 2024. Synthesis of aluminum alginate/graphene oxide/boehmite biopolymeric nanohybrid for the decontamination of Cu(II) and 2-chlorophenol. *Journal of the J. Taiwan Inst. Chem. Eng.* 161, 105515.
- [47] K. Jin-tao, T. Zheng-chang, Z. Yu-feng, Adsorption of Copper (II) by magnesium hydroxide modified Prunus mira Koehne shell activated carbon, *Adsorpt. Sci. Technol.* 42 (2024) 02636174241256848. <https://doi.org/10.1177/02636174241256848>.
- [48] Taleb M.A., Kumar R. and Barakat M.A., 2023. Multifunctional carboxymethyl cellulose/graphene oxide/polyaniline hybrid thin film for adsorptive removal of Cu(II) and oxytetracycline antibiotic from wastewater. *Int J Biol Macromol.* 253, 126699.
- [49] Taleb M.A., Kumar R., Al-Rashdi A.A., Seliem, M.K. and Barakat M.A., 2020. Fabrication of SiO₂/CuFe₂O₄/polyaniline composite: a highly efficient adsorbent for heavy metals removal from aquatic environment. *Arab J Chem*, 13(10), pp.7533-7543.
- [50] N.A. Öztaş, A. Karabakan, Ö. Topal, Removal of Fe(III) ion from aqueous solution by adsorption on raw and treated clinoptilolite samples, *Microporous Mesoporous Mater.* 111 (2008) 200–205. <https://doi.org/https://doi.org/10.1016/j.micromeso.2007.07.030>.
- [51] T. Bakalár, M. Kaňuchová, A. Girová, H. Pavolová, R. Hromada, Z. Hajduová, Characterization of Fe(III) Adsorption onto Zeolite and Bentonite, *Int. J. Environ. Res. Public Health.* 17 (2020). <https://doi.org/10.3390/ijerph17165718>.
- [52] C. Quintelas, Z. Rocha, B. Silva, B. Fonseca, H. Figueiredo, T. Tavares, Removal of Cd(II), Cr(VI), Fe(III) and Ni(II) from aqueous solutions by an E. coli biofilm supported on kaolin, *Chem. Eng. J.* 149 (2009) 319–324. <https://doi.org/https://doi.org/10.1016/j.cej.2008.11.025>.
- [53] V. Lugo-Lugo, C. Barrera-Díaz, F. Ureña-Núñez, B. Bilyeu, I. Linares-Hernández, Biosorption of Cr(III) and Fe(III) in single and binary systems onto pretreated orange peel, *J. Environ. Manage.* 112 (2012) 120–127. <https://doi.org/https://doi.org/10.1016/j.jenvman.2012.07.009>.